https://doi.org/10.5194/egusphere-2025-3677
Preprint. Discussion started: 6 October 2025

Seasonal forecasting of water table elevation in shallow unconfined aquifers with a case study in the Umbria Region, Italy

Miriam Saraceni [1], Gregorio Gazzetta [2,5], Lorenzo Silvestri [3], Bruno Brunone [2], Silvia Meniconi [2], and Paolina Bongioannini Cerlini [4]

[1]CIRIAF, Inter-University Centre for Research on Pollution and the Environment, 'Mauro Felli', University of Perugia, Perugia, Italy
[2]Department of Civil and Environmental Engineering, University of Perugia, Perugia, Italy
[3]Department of Engineering Enzo Ferrari, University of Modena and Reggio Emilia, Modena, Italy
[4]Department of Physics and Geology, University of Perugia, Perugia, Italy
[5]AcegasApsAmga, SpA, Trieste, Italy

Correspondence: Miriam Saraceni (miriam.saraceni@unipg.it)

Abstract. Accurate seasonal forecasting of water table elevation is critical for effective water resource management in unconfined aquifers, particularly under climate variability and anthropogenic pressures. This study presents a novel methodology for predicting water table elevation on seasonal timescales by coupling reanalysis and seasonal forecast data of soil moisture with a calibrated nonlinear transfer model. The approach leverages ERA5 reanalysis and SEAS5 seasonal forecasts to estimate flux toward the aquifer and forecast water table elevation. A case study in the Umbria Region of central Italy demonstrates the model's ability to simulate and predict monthly water table fluctuations. Two modeling strategies are compared: a static calibration approach (OPT_1) and a dynamic calibration approach (OPT_2), where model parameters are updated by considering different time periods. Both options yielded skillful forecasts across lead times of 1 to 6 months, with OPT_2 showing slightly improved stability in forecast performance metrics. Results confirm the feasibility of incorporating seasonal climate forecasts into operational groundwater prediction frameworks. As expected, forecast accuracy is limited by the skill of precipitation predictions, especially during autumn and winter. The proposed framework lays the groundwork for anticipatory aquifer management and early warning systems under evolving hydroclimatic conditions.

1 Introduction

About 97 % of liquid freshwater resources on Earth is due to groundwater (WHO, 2006; Healy, 2010). Accordingly, groundwater resources are of a paramount importance for preserving ecosystems and assuring water supply. As examples, groundwater provides river discharge as well as it contributes significantly to water budget in lakes. Its critical role in the drinkable water management derives from the fact that an aquifer behaves as a reservoir assuring water with a much better quality with respect to surface water (Brussolo et al., 2022).

From both the quantitative and qualitative point of view, potential of an unconfined aquifer is determined by the elevation of the water table. Such a quantity derives from the entity of groundwater recharge, a quantity very difficult to measure directly, that is mainly due to precipitation infiltrating the soil surface. In some cases, the role of the so-called interaquifer flow – i.e.,

https://doi.org/10.5194/egusphere-2025-3677
Preprint. Discussion started: 6 October 2025

the one from an unconfined aquifer across a confining bed to an underlying aquifer – cannot be neglected (Healy, 2010).

In unconfined aquifers, groundwater recharge, R_R, in a given time interval, Δt, can be obtained by measuring the related water table fluctuation, Δh_w, according to the following water budget relationship:

$$R_R = S_y \frac{\Delta h_w}{\Delta t} \quad (1)$$

where S_y = specific yield, a quantity provided by in-situ tests. However, strong uncertainty in the evaluation of S_y (Healy, 2010), on one side, and the fact that for the purposes of water systems managers, the quantity that is directly relevant is the elevation of the aquifer water table, h_w, on the other, suggest focussing the attention on the behaviour of h_w. In fact, to give a simple example, the discharge that can be withdrawn from a well by a pump with a given power depends on the prevalence and then on the water table elevation. In this perspective, two issues must be addressed. The first one, an essential step within the strategy for the aquifer management, concerns the development of a numerical model that allows simulating the behaviour of the water table elevation. Such an issue is of great relevance as it testifies the capability of capturing the main features of the behaviour of the investigated aquifer. The aim of the second issue, much more challenging indeed, is the development of a model for forecasting the behaviour of the water table elevation in the next few months to adopt appropriate management strategies.

The classical approach for the development of a numerical model simulating the behaviour of the water table elevation is based on the use of the Darcy equation with the aquifer parameters provided by field pumping tests. Recently, as an alternative option, the joint use of h_w measurements from piezometers and soil moisture data from reanalysis has been proposed (Bongioannini Cerlini et al., 2021). The appeal of this approach stems from two features. The first one is that many local, state and federal agencies maintain databases of water table elevation, a quantity easy to measure. The second feature is that reanalysis covers all the world and is fully open access. As the same modeling system producing reanalysis may also provide the seasonal forecasting system, the forecasted soil moisture can be used to forecast the water table elevation by means of the refined numerical model. This approach is based on the encouraging results obtained in Silvestri et al. (2025), where the consistent assessment of monthly soil moisture anomalies' seasonal forecast skill in the central Mediterranean (including Umbria, Italy) has been carried out. Accordingly, as it will be discussed in detail in the next sections, in this paper, the possible application of seasonal forecasts of soil moisture for groundwater management and water table elevation forecast is explored.

This paper is organized as follows. Section 2 presents the procedure proposed for forecasting the water table elevation based on the seasonal forecast of the soil moisture and the model refined for the simulation of h_w based on the joint use of piezometer measurement and reanalysis data. In Section 3, the procedure is used to forecast the water table elevation of a piezometer in the Umbria Region, Italy. Key results and future research directions are highlighted in the Conclusions.

2 Seasonal Forecasting Procedure

The proposed procedure is based on the joint use of the values of the water table elevation of the aquifer, h_w, measured at piezometers, and soil moisture, θ, from reanalysis datasets and seasonal forecasts. The entire procedure is outlined in Fig. 1.

https://doi.org/10.5194/egusphere-2025-3677
Preprint. Discussion started: 6 October 2025

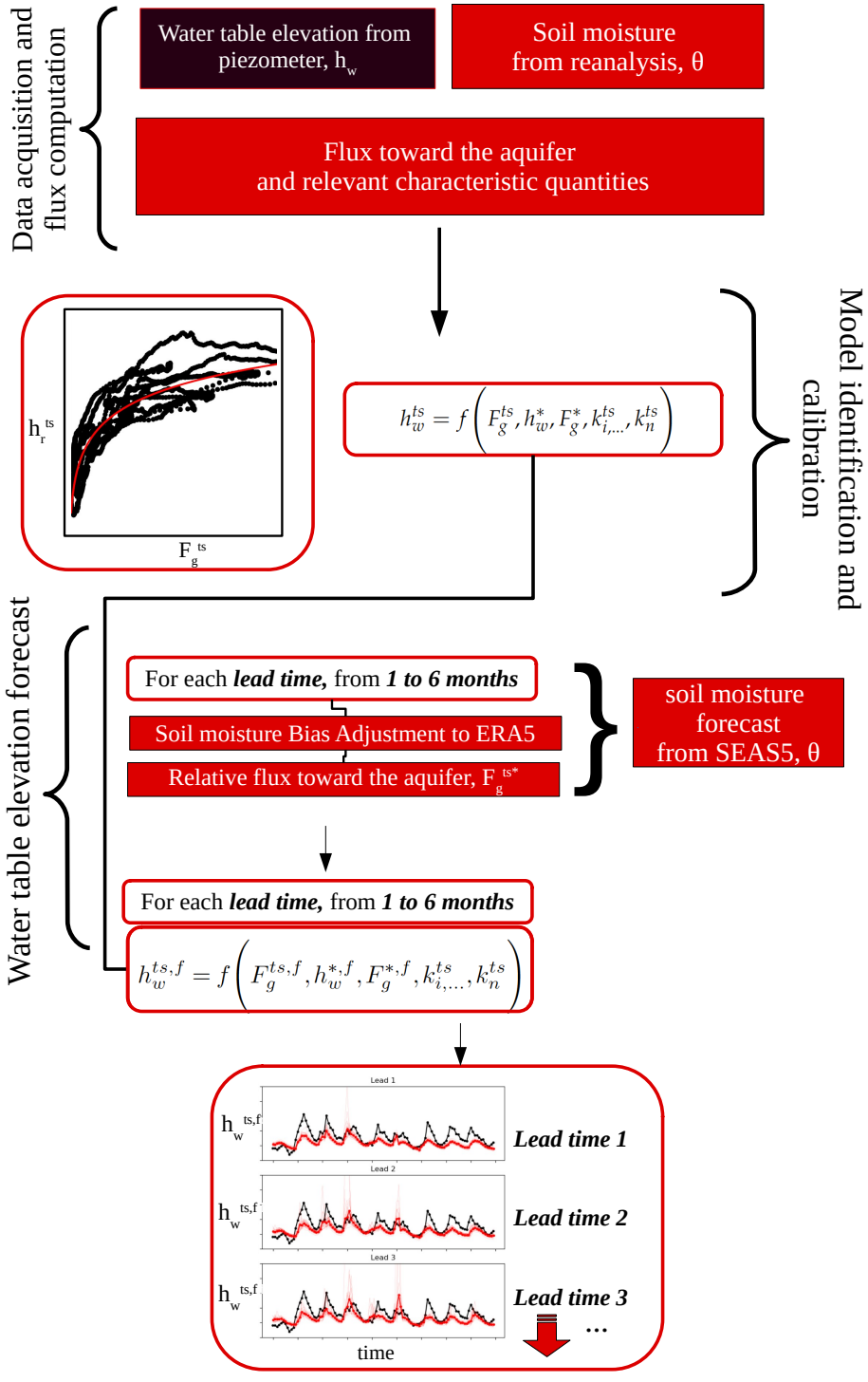

Figure 1. Procedure flowchart (option #1, OPT_1).

https://doi.org/10.5194/egusphere-2025-3677
Preprint. Discussion started: 6 October 2025

Step #1 of the procedure (*Data acquisition and preliminary computations*) includes three actions. The first one is the identification of the piezometers where the water table elevation is measured. For the chosen reanalysis, the second action concerns the selection of the most appropriate soil moisture reanalysis datasets (in most cases, the reanalysis data grid point closest to the piezometers is used). Within the third action, the flux towards the aquifer, F_g, is evaluated by using the soil moisture datasets and soil parameters from the reanalysis.

For a given time scale, ts, within step #2 (*Model identification and calibration*), the relationship between h_w and F_g is identified and the model parameters are evaluated.

In step #3 (*Water table elevation forecast*), the forecasting of the water table elevation is executed by means of the calibrated model and the seasonal forecasting system of soil moisture associated to the used reanalysis. In successive subsections, the above steps of the proposed procedure are described in detail.

2.1 Step #1: Acquisition of piezometer and reanalysis datasets and flux towards the aquifer evaluation

In the region of interest, within a procedure for the identification of available high-quality environmental data (Silvestri et al., 2022), the selection of the piezometers can be based on the criteria discussed in Bongioannini Cerlini et al. (2021). In particular, the presence of disturbances induced by human activities, and the mean depth of the water table, D, relative to ground level must be considered. Regarding the first criterion, the water table fluctuations are analyzed to detect possible significant oscillations due to, as an example, irrigation. Regarding the second criterion, the mean water table depth must range between 4 m and 10 m. The lower bound is related to the length of the soil column, d, explored in the hydrology model providing the reanalysis (as pointed out below, in the reanalyses, the largest value of d is equal to 2.89 m). The upper bound represents a reasonable maximum depth for shallow aquifers, where infiltration behaves as the primary recharge mechanism. According to Seibert et al. (2003), this depth range ensures that the interaction between the vadose zone and the aquifer is largely unidirectional.

The choice of reanalysis is guided by several factors depending on the specific application considered but also region and time scale (Lorenz and Kunstmann, 2012; Li et al., 2020). For the management of aquifers, in Bongioannini Cerlini et al. (2023) it has been pointed out that the choice of reanalysis can be based on features such as the relevance of the spreading of the water table elevation, soil model used in the hydrological model (Brunone et al., 2003), length of the explored soil column, and spatial resolution. Accordingly, in this paper, ECMWF Reanalysis v5 (hereafter, ERA5), provided by the European Centre for Medium-Range Weather Forecasts (ECMWF), is used (Hersbach et al., 2020).

ERA5 is generated by the Integrated Forecasting System (IFS) model (specifically, the CY42R1 version). The land surface component employs the H-TESSEL model (Balsamo et al., 2009), which directly interacts with the atmosphere. Within ERA5, observations are assimilated every 12 hours by a four-dimensional variational (4D-Var) data assimilation scheme. The combination of ERA5's fine horizontal resolution (0.25^o or approximately 31 km), along with advancements in physical modeling and data assimilation techniques, establishes this dataset as one of the most robust and physically consistent global soil moisture reanalyses (Balsamo et al., 2009).

To derive the initial soil moisture conditions, IFS incorporates a simplified Extended Kalman Filter (De Rosnay et al., 2013).

https://doi.org/10.5194/egusphere-2025-3677
Preprint. Discussion started: 6 October 2025

This process relies on two primary sources of observational data (Albergel et al., 2012): surface-level measurements of temperature and relative humidity from synoptic weather stations (SYNOP) at 2 meters above ground level (commonly referred to as screen-level data), and soil moisture estimates from the MetOp-A and MetOp-B Advanced Scatterometer (ASCAT) satellite sensors. While screen-level observations provide an indirect relationship to soil moisture, satellite-based data offer a more direct assessment of surface soil moisture. However, since satellite observations are limited only to the uppermost soil layers (Albergel et al., 2012), deeper root-zone moisture levels are inferred by propagating this surface information downward using the H-TESSEL hydrological model. Specifically, the dynamics of the soil moisture, θ, in m^3m^{-3}, is simulated by means of the diffusive formulation of the Richard's equation:

$$\frac{\partial\theta}{\partial t} = -\frac{\partial}{\partial z}\left(\lambda(\theta)\frac{\partial\theta}{\partial z} - \gamma(\theta)\right) + S_\theta \tag{2}$$

where t = time, z = depth below the ground surface, $\lambda(\theta)$ = hydraulic diffusivity, and $\gamma(\theta)$ = hydraulic conductivity; and S_θ accounts for all soil moisture sources and sinks, such as evaporation, plant water uptake, surface runoff, and precipitation. ERA5 evaluates the hydraulic parameters λ and γ using the analytical expressions proposed by Van Genuchten (1980):

$$\gamma = \gamma_s \frac{\left[\left(1+(\alpha p)^n\right)^{1-1/n} - (\alpha p)^{n-1}\right]^2}{\left(1+(\alpha p)^n\right)^{(1-1/n)(l+2)}} \tag{3}$$

$$\lambda = \gamma\frac{\partial p}{\partial\theta} \tag{4}$$

where the subscript s indicates the saturated conditions, α, n and l are empirical parameters that depend on soil texture. The pressure head, p, is related to soil moisture via:

$$\theta = \theta_r + \frac{\theta_s - \theta_r}{\left(1+(\alpha p)^n\right)^{(1-1/n)}} \tag{5}$$

where θ_r, the residual moisture content, and θ_s, the saturated soil moisture, are constant parameters that depend on the soil texture. In ERA5, soil texture is spatially variable but temporally invariant and vertically homogeneous within each soil column. There are seven soil texture classes employed in the model (i.e., sea, coarse, medium, medium fine, fine, very fine, and organic), with their associated parameter values provided in Table 1 of Balsamo et al. (2009). The soil parameters, texture, α, n, l, θ_r and θ_s are related to the chosen grid point.

In ERA5, the number and the depth of soil layers in each soil column is four: z = 0.07 m (soil layer #1), 0.28 m (soil layer #2), 1.00 m (soil layer #3), and 2.89 m (soil layer #4), respectively. At the upper boundary of the soil column, conditions are defined by the surface energy balance. Conversely, at the bottom of the soil column, ERA5 assumes a free drainage condition, with the flux towards the aquifer, F_g, given by:

$$F_g = \gamma_{bot} \tag{6}$$

where γ_{bot} = hydraulic conductivity of the deepest soil layer (z = 2.89 m).

https://doi.org/10.5194/egusphere-2025-3677
Preprint. Discussion started: 6 October 2025

2.2 Step #2: Model identification and calibration

Once the time scale, ts, has been chosen, the related aggregated flux towards the aquifer, F_g^{ts}, and representative value of the water table elevation, h_w^{ts}, are computed (as an example, the monthly flux and mean value respectively). To assess the connection between these quantities, a cross-correlation analysis using the Spearman rank correlation coefficient, *R*, is executed (Zar, 2005). This is a nonparametric (distribution-free) approach to the correlation between two sets of data, where each set may be ranked in order of magnitude. Then, the standard Pearson's correlation coefficient is calculated on the two sets of ranks. As a result of the analysis, the model structure is identified as:

$$h_w^{ts} = f\left(F_g^{ts}, h_w^*, F_g^*, k_{i,\ldots}^{ts}, k_n^{ts}\right) \tag{7}$$

where h_w^* and F_g^* are reference values of the water table elevation and flux towards the aquifer, respectively, and $k_{i,\ldots}^{ts}, k_n^{ts}$ are the model parameters. Equation (7) can be reformulated in a normalized, dimensionless form.

2.3 Step #3: Water table elevation forecast

As seasonal forecast of soil moisture at the selected time scale, the ECMWF fifth-generation seasonal forecasting system, SEAS5 (Johnson et al., 2019), is used. As such, SEAS5 comes from the same modeling system that produces ERA5 reanalysis, making it suitable in this context. Indeed, seasonal forecast outputs from SEAS5 originate from a separate model version, featuring distinct initialization procedures, data assimilation techniques, and horizontal resolutions. Precisely, SEAS5 is built upon cycle 43r1 of the Integrated Forecasting System (IFS) and incorporates a fully coupled model including atmospheric, land surface, oceanic, and sea-ice components. The atmospheric model operates at a horizontal resolution of approximately 36 km (O320 grid) with 91 vertical levels. The ocean component utilizes the ORCA model (0.25° resolution) with 75 vertical levels. Land processes are simulated through the H-TESSEL scheme (Balsamo et al., 2009), while the LIM2 model (Fichefet and Maqueda, 1997) represents sea-ice dynamics. The same as ERA5 approach regarding the soil type is applied within the SEAS5 seasonal forecasting system. Furthermore, the number and depth of soil layers in each column in ERA5 are the same in SEAS5. The atmosphere and land surface initialization relies on ECMWF operational analyses, whereas oceanic and sea-ice states are initialized using OCEAN5 (Zuo et al., 2019), which combines ORAS5 ocean reanalysis with daily ocean analysis from OCEAN5-RT (see Johnson et al., 2019, for further details).

SEAS5 comprises both reforecasts (meaning *retrospective forecasts*), consisting of 25 ensemble members, and forecasts, consisting of 51 members. To ensure consistency across the entire dataset, only the first 25 members of the forecasts are retained. SEAS5 reforecasts cover only the period from 1993 to 2016, and forecasts have been produced afterward. The distinction arises because SEAS5 became operational in 2017 and real-time forecasts have been produced since then. Reforecasts are generated to extend the dataset of seasonal forecasts, improving calibration. In terms of lead times, each forecast is produced with a 7-month lead time and is initialized at the start of each month.

Seasonal forecast output needs to undergo a bias adjustment procedure in order to adhere to the climatological values. The

https://doi.org/10.5194/egusphere-2025-3677
Preprint. Discussion started: 6 October 2025

method used in this paper is the simple mean and variance adjustment (MVA) method, as described in Manzanas et al. (2019). Precisely, each member's mean and variance over each grid point is bias-adjusted with respect to the ERA5 observation mean and variance over a climatologically chosen period, in the following form:

$$\theta'_k(l,m,y,j) = (\theta_k(l,m,y,j) - \hat{\theta_k}(l,m))\frac{\sigma_o(m)}{\sigma_f(l,m)} + \overline{\theta^o_k}(m) \quad (8)$$

where θ'_k = bias-adjusted soil moisture, l = forecast lead time, m = forecast month, j = index indicating the ensemble member, y = year, and k = soil layer, $\hat{\theta_k}(l,m)$ = ensemble and time average of forecasts for each lead time and month over the reference period, $\sigma_f(l,m)$ = standard deviation of the complete ensemble for each lead time and month over the reference period, $\sigma_o(m)$ = standard deviation of all observations for the considered month over the reference period, and $\overline{\theta^o_k}$ = time average of all observations for the considered month over the reference period. The bias adjustment is computed for each forecast lead time. In this way, the bias and variance adjustment takes into account both the forecast month and forecast lead time, which is found to be beneficial in previous work (Kumar et al., 2014). Although the simplest among different methods, in Manzanas et al. (2019) it is demonstrated that the MVA method represents a good compromise between computational cost and performance. This is particularly relevant since the final aim of this study is to develop real-time applications for climate services and water systems management.

After obtaining the model-calibrated parameters for a validation period, $k^{ts}_{i,\dots}, k^{ts}_n$ of Eq. (7), the seasonal forecast of the water table elevation is carried out as outlined below:

1. the SEAS5 soil moisture, θ, is bias-adjusted to match the ERA5 climatology using the method described above for each lead time (in the analysis, lead times ranging from 1 to 6 months are considered);
2. the SEAS5 θ time series closest to the piezometer location is selected to calculate the flux toward the aquifer, F^{ts}_g, as detailed in Section 2.1 for each lead time;
3. the flux toward the aquifer computed for the forecasting period is used in the calibrated model to forecast the water table elevation by Eq. (7).

The above process implies choosing a fixed climatological period for the observation used for the calibration (we will refer to the first process as the *static* option or option #1, OPT_1). A variation of OPT_1 consists of dynamically updating the observation period used for calibration, extending it in a progressive way as time passes, increasing it in six-month increments. This allows for recalculating the parameters every six months and dynamically repeating the forecast. This modified forecasting process is referred to below as the *dynamic* option or option #2, OPT_2.

3 The case study of Umbria Region

In this Section, the proposed procedure is used for forecasting the water table elevation of a shallow unconfined aquifer in the Umbria Region, Italy. The piezometer analyzed as a preliminary case study in this paper, the *P1-Pistrino* piezometer, belongs to

https://doi.org/10.5194/egusphere-2025-3677
Preprint. Discussion started: 6 October 2025

the regional piezometric monitoring network, managed by the Regional Environmental Protection Agency [Agenzia Regionale per la Protezione Ambientale (ARPA)] (ARPA Umbria, 2008) (Fig. 2), established in 2001. This piezometer fulfills the relevant criteria identified in Section 2.1. Its location is shown in Fig. 2 and its characteristics are summarized in Table 1 whereas the
180 applicable soil textures, soil type, and their corresponding parameters from ERA5 are listed in Table 2.

The available dataset provides daily measurements of the water table elevation, h_d^w, which is computed as the median of hourly readings after executing a quality control process. Specifically, at least three hourly observations are required to estimate h_d^w (ARPA Umbria, 2008). According to the needs of the groundwater resources management, monthly mean values, h_m^w, are considered.

Table 1. P1-Pistrino piezometer, from the ARPA Umbria network, selected as a case study. Columns from left to right: identification number, P, and name of piezometer; latitude and longitude (in decimal degrees) and height (in m a.s.l. as extracted from the digital elevation model); the corresponding ERA5 grid point and aquifer; starting year of measurements; mean depth of the water table (m) relative to ground level; standard deviation of the water table measurements (m).

Name	Lat	Lon	Height	G	Aquifer	Start	D	$\sigma_{h_w^d}$
P1-Pistrino	43.5099	12.1475	294	G1	AQ1	2001	4.5	0.6

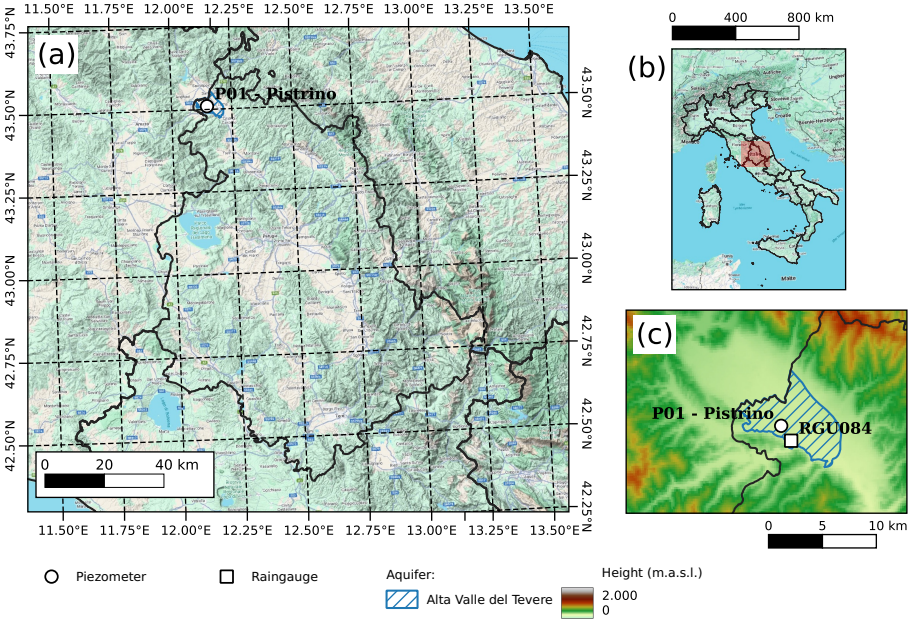

Figure 2. In (a) map of the Umbria Region, Italy (in (b)) with the aquifer area and the ERA5 grid; in (c) the Umbria region weather station measuring precipitation (RGU084) and the piezometer, P1-Pistrino.

https://doi.org/10.5194/egusphere-2025-3677
Preprint. Discussion started: 6 October 2025

Accordingly, in the adopted methodology, the flux toward the aquifer is temporally aggregated to obtain the monthly values, F_g^m.

Table 2. Van Genuchten soil parameters for the land texture type considered in the analyzed grid point of Fig. 2.

Soil Texture	α	l	n	γ_s	θ_s	θ_r
Medium (loamy soil)	3.14 (m^{-1})	-2.342	1.28	1.16(10^{-6} m s^{-1})	0.439	0.010

For the considered piezometer, in Bongioannini Cerlini et al. (2017, 2021) the following relationship between h_w^m and F_g^m has been obtained:

$$h_w^m = h_w^{max} - \sigma_w^m \left(k_{log}^m \log\left(\frac{F_g^{max}}{F_g^m}\right) + k_{lin}^m \left(\frac{F_g^{max} - F_g^m}{F_g^{max}}\right)\right) \tag{9}$$

where h_w^{max} and F_g^{max} are selected as reference values with h_w^{max} being the 99th percentile of h_w and F_g^{max} the absolute maximum value of F_g; σ_w^m is the standard deviation of the monthly water table elevation. k_{lin}^m, k_{log}^m are the model parameters defining the relative influence of non-linear and linear components in the relationship between h_w^m and F_g^m (Fig. 3a). They have been obtained through non-linear least squares fitting. Equation (9) can also be written in a dimensionless way as:

$$h_r^{m*} = k_{log}^m \log(F_g^{m*}) + k_{lin}^m (1 - \frac{1}{F_g^{m*}}) \tag{10}$$

where $h_r^{m*} = (h_w^{max} - h_w^m)/\sigma_w^m$ = dimensionless water table elevation, and $F_g^{m*} = F_g^{max}/F_g^m$ = dimensionless flux towards the aquifer. This dimensionless framework allows for direct comparison of groundwater dynamics across piezometers with different behaviors.

In this paper, the calibration of the k_{log}^m and k_{lin}^m parameters has been executed by means of the piezometric observations and ERA5 reanalysis soil moisture from 2001 to 2012 to be consistent with previous work (Bongioannini Cerlini et al., 2023), and to take as calibration period nearly half of the total observed period. The performance assessment of modeling the water table elevation for the P1-Pistrino piezometer is reported in Table 3 and Fig. 3b.

Table 3. Monthly statistical properties of water table observations and interpolation parameters. Columns from left to right: piezometer identifier; maximum Spearman coefficient R_{max}; h_w^{max}; F_g^{max}; and model parameters, k_{log}^m and k_{lin}^m.

Piezometer	R_{max}	h_w^{max}(m)	F_g^{max}(m)	k_{lin}^m	k_{log}^m
P1-Pistrino	0.807	291.1	0.017	1.87	0.786

The obtained model is then used to forecast the water table elevation by using the seasonal forecasting system, SEAS5. Each forecast consists of multiple ensemble members and lead times. Seasonal reforecasts from 2001 to 2016 and seasonal forecasts from 2016 to 2021 have been used. The period considered for the seasonal forecasting procedure spans 20 years from 2001 to 2021, while the reference period considered for evaluating the monthly climatology and standard deviation ranges from 2001

https://doi.org/10.5194/egusphere-2025-3677
Preprint. Discussion started: 6 October 2025

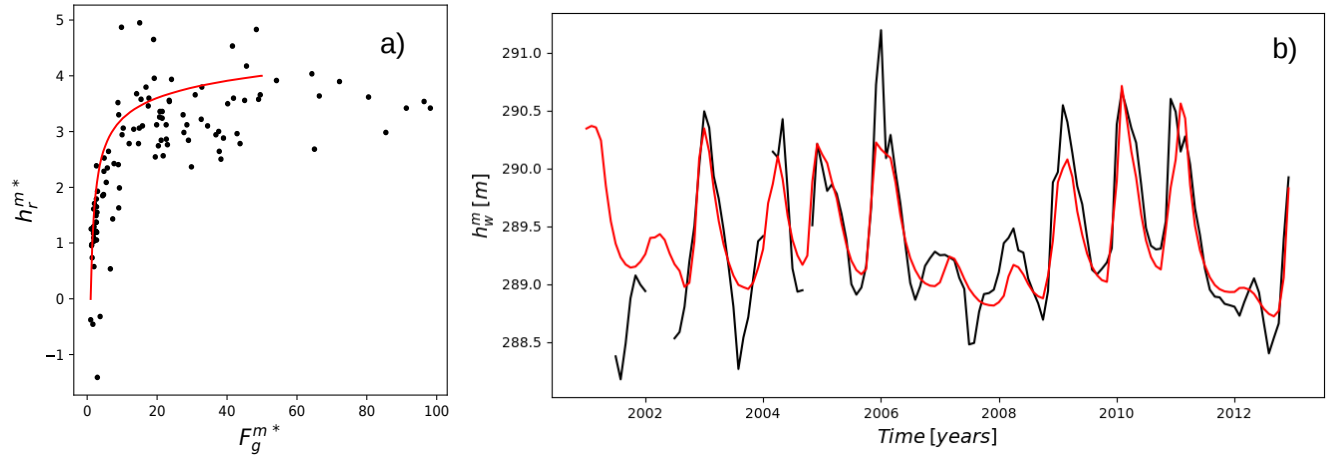

Figure 3. In (a) scatter plot of monthly dimensionless water table elevation, vs. monthly dimensionless groundwater fluxes, from 2001 to 2012 for P1-Pistrino piezometer. Red curves represent a logarithmic-linear relationship of Eq. (7), with parameters reported in Table 3. In (b), the simulations of the daily water table elevation (in m a.s.l.) of P1-Pistrino piezometer as given by the ERA5 reanalyses (red and black lines indicate the simulated and measured values, respectively).

to 2016, the same period considered for the bias adjustment of the seasonal forecast of soil moisture. The forecasting process is then carried out as follows. After obtaining the parameters k_{log}^m and k_{lin}^m based on the calibration of the relationship between F_g^{m*} and h_r^{m*} in the period from 2001 to 2012 (the calibration period), the seasonal forecast of the water table elevation is carried out following the already described OPT_1. For the sake of clarity, for each lead time, the steps of OPT_1 are synthesized below:

1. the SEAS5 soil moisture θ is bias-adjusted to match the ERA5 climatology (from 2001 to 2016) using the method described in Section 2.3;
2. the SEAS5 θ time series closest to the piezometer location is selected to calculate F_g^{m*} from 2012 to 2021 for each lead time;
3. F_g^{m*} computed from 2012 to 2021 is used with the parameters k_{log}^m and k_{lin}^m to forecast the water table elevation in the following months using Eq. (10).

As mentioned above, the alternative option, OPT_2, consists of dynamically updating the calibration period, extending it progressively from 2001–2012 to 2001–2021, increasing it in six-month increments from 2012 onward (e.g., validating up to 2012-06, then up to 2012-12, and so on). This allows for recalculating the parameters k_{log}^m and k_{lin}^m every six months and dynamically repeating the forecast (e.g., simulating from 2012-06, then from 2012-12, and so on). Given that the bias adjustment procedure stays the same, OPT_2 can be summarized as:

https://doi.org/10.5194/egusphere-2025-3677
Preprint. Discussion started: 6 October 2025

1. the SEAS5 θ time series closest to the piezometer is selected to compute the groundwater flux, F_g^{m*}, from 2012 to 2021 for each lead time, with a six-month step;

2. the groundwater flux computed from 2012 to 2021 is used with the parameters k_{log}^m and k_{lin}^m to forecast the water table elevation in the following months using Eq. (10), extending the validation period and shifting the simulation window every six months.

3.1 Forecast performance evaluation

For checking the forecast performance, some statistical indices are analyzed. Precisely, the Pearson's correlation coefficient, r^2:

$$r^2 = \frac{\sum_i^N (f_i - \mu_f)(o_i - \mu_o)}{\sigma_f \sigma_o} \tag{11}$$

where N is the number of values, f_i are the forecasted values, o_i are the observations, σ_f and σ_o are the standard deviations of the forecasts and observations, respectively, and μ_f and μ_o are the forecasts and observations means, respectively; the Root Mean Squared Error, RMSE:

$$RMSE = \sqrt{\frac{1}{N}\sum_i^N (f_i - o_i)^2} \tag{12}$$

the Mean Absolute Error, MAE, defined as the absolute value of the Mean Bias, MB:

$$MB = \frac{1}{N}\sum_i^N (f_i - o_i) \tag{13}$$

the Spearman Rank correlation, and the Kling–Gupta efficiency parameter, KGE, (Gupta et al., 2009) defined as:

$$KGE = 1 - \sqrt{(r^2 - 1)^2 + (\frac{\sigma_f}{\sigma_o} - 1)^2 + (\frac{\mu_f}{\mu_o} - 1)^2} \tag{14}$$

All indices have been evaluated in the forecasted period, from 2012 to 2020.

4 Results

4.1 Water table elevation forecast by option #1 (OPT_1)

Figures from 4 to 6 present the results of water table elevation monthly forecasts at the P1-Pistrino piezometer site using the static calibration approach, OPT_1. In this option, the relationship between the ERA5-derived flux towards the aquifer and the observed water table elevation has been calibrated over the 2001–2012 period, and then applied to SEAS5 seasonal forecasts from 2012 onward. The performance of OPT_1 is reported in Table 4 for the forecasted period.

https://doi.org/10.5194/egusphere-2025-3677
Preprint. Discussion started: 6 October 2025

Table 4. Performance parameters of OPT_1.

Piezometer	Lead Time	KGE	RMSE (m)	MAE (m)	R	r^2
P1-Pistrino	Lead 1	0.6	0.4	0.3	0.8	0.7
	Lead 2	0.6	0.6	0.5	0.7	0.7
	Lead 3	0.5	0.7	0.4	0.7	0.4
	Lead 4	0.5	0.7	0.5	0.6	0.6
	Lead 5	0.5	0.6	0.5	0.6	0.5
	Lead 6	0.4	0.6	0.4	0.6	0.5

The plots demonstrate the temporal consistency and predictability of the groundwater dynamics under different seasonal starting points (from lead time 1 to 6). The predicted ensemble mean trajectories (red thick lines in Fig. 4) reasonably track the observed evolution of h_w^m (black line). This behavior suggests that the calibrated model retains skill across multiple lead times. This is confirmed by the stable values of the KGE, the Spearman, and linear correlation reported in Table 4. While the RMSE is skewed towards the highest discrepancy, the mean absolute error (MAE) is about 0.5 m, indicating a reasonable forecasting error. It is also notable that, as expected, while uncertainty increases with lead time, the forecasts generally maintain the observed seasonal trend and amplitude.

https://doi.org/10.5194/egusphere-2025-3677
Preprint. Discussion started: 6 October 2025

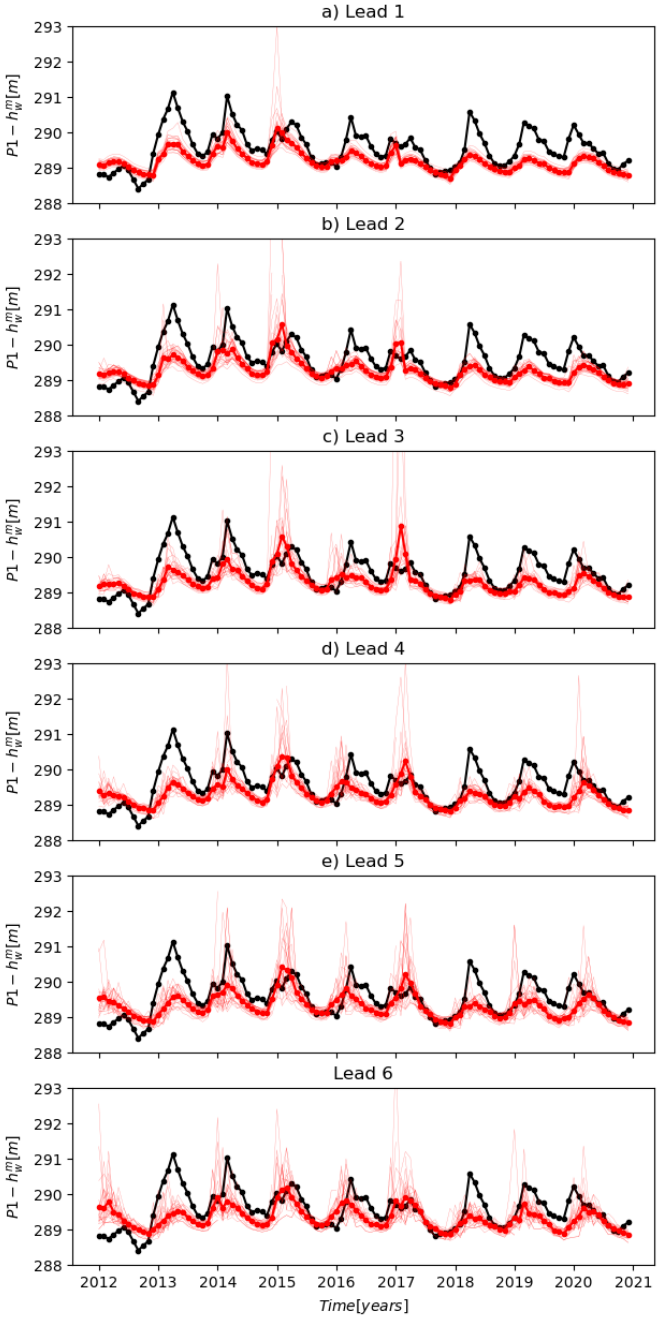

Figure 4. From (a) to (f) the forecast of the monthly water table elevation, h_w^m (in m a.s.l.) of P1-Pistrino piezometer as given by the SEAS5 seasonal forecast (red and black lines indicate the forecasted and measured values, respectively) for each lead time, from 1 month to 6 months. The thick red line is the ensemble average, whereas the thinner ones represent each ensemble member.

https://doi.org/10.5194/egusphere-2025-3677
Preprint. Discussion started: 6 October 2025

Two focused assessments of the forecasts have been examined in detail: between January and May 2015 (Fig. 5) and from June to October 2015 (Fig. 6). The results highlight the variability in forecast performance as a function of both initialization month and forecast horizon. In Fig. 5, a gradual increase in forecast uncertainty is evident as the lead time progresses, consistent with the degradation of predictability typically observed in seasonal hydrological models. Despite this, the forecast ensemble maintains a strong coherence with the observed signal, confirming the robustness of OPT_1.

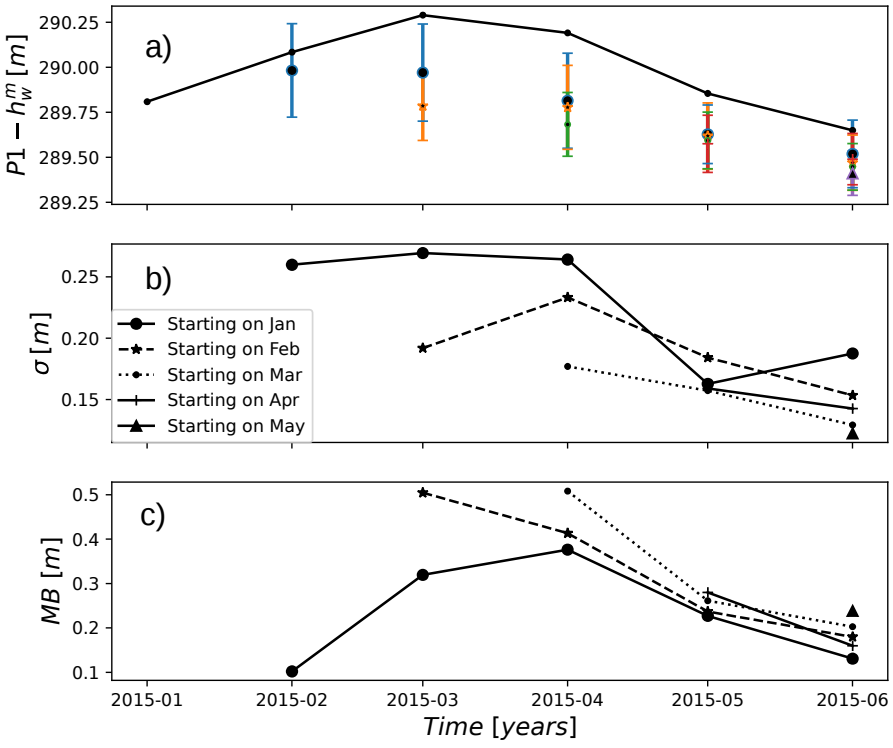

Figure 5. Water table elevation forecast assessment for the period 2015/06 to 2015/11: (a) the forecasted (coloured points) and the observed water table elevations; (b) the ensemble spread, reported as the standard deviation, for each forecasted period; (c) the mean bias (MB) of each forecast.

In contrast, Fig. 6 exhibits a more stable predictive structure across shorter lead times. The reduced forecast error and lower ensemble spread in this case suggest that the model performs better in dry periods when soil moisture effects dominate the groundwater response. This may reflect the limited influence of external forcings such as intense precipitation events during this period, which reduces the variability not captured by the model structure.

https://doi.org/10.5194/egusphere-2025-3677
Preprint. Discussion started: 6 October 2025

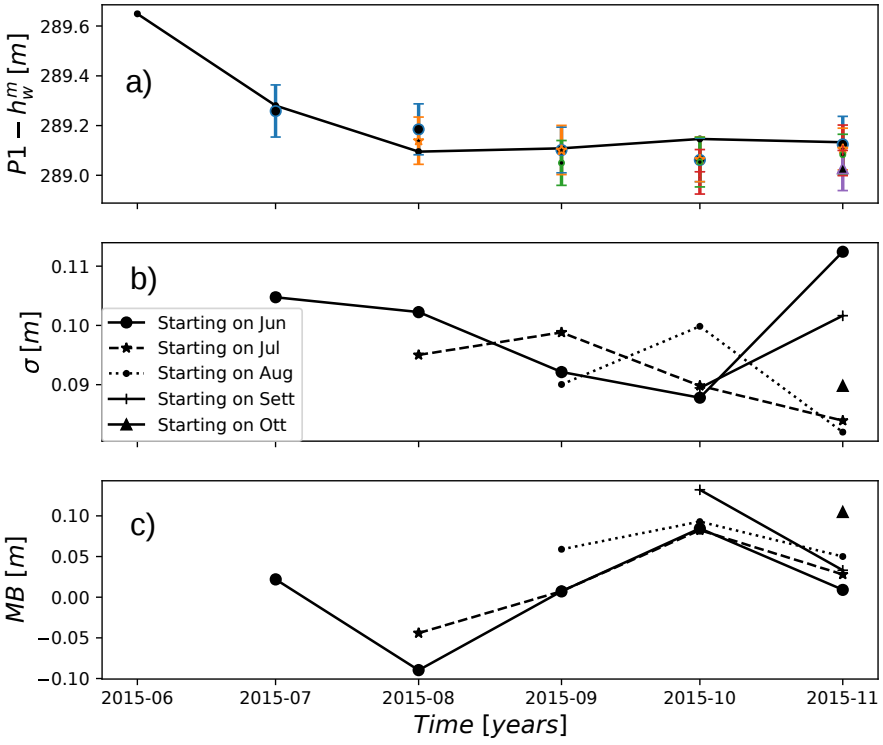

Figure 6. Water table elevation forecast assessment for the period 2015/01 to 2015/06: (a) the forecasted (coloured points) and the observed water table elevations; (b) the ensemble spread, reported as the standard deviation, for each forecasted period; (c) the mean bias (MB) of each forecast.

The average ensemble of h_w^m remains below 0.25 m across all runs for the winter-to-spring period and below 0.1 m for the summer-to-fall period. This indicates a robust forecast capability with a slightly better alignment with soil moisture conditions during the wet-to-dry transition and a more effective representation of the recharge processes in spring and early summer. This is also underlined by the different MB in the two periods. While in the winter to spring period the MB can go up to 0.5 m (Fig. 5c), in the summer to fall period it oscillates between -0.10 m to 0.10 m (Fig. 6c). The predictive performance appears to be fairly consistent regardless of the initialization month, which reinforces the utility of monthly SEAS5 products for seasonal-scale groundwater applications. The results confirm the model's ability to reproduce the general shape and magnitude of seasonal water table elevation even during drier months. However, a slight positive bias can be observed for earlier initializations (January–February), suggesting that future improvements could consider temporal correction factors, as done by OPT_2 reported below.

https://doi.org/10.5194/egusphere-2025-3677
Preprint. Discussion started: 6 October 2025

4.2 Water table elevation forecast by option #2 (OPT_2)

Fig. 7 presents the results obtained through the dynamically updated forecasting approach (OPT_2), which differs from OPT_1 by updating the hydrological model parameters k_{log}^m and k_{lin}^m every six months throughout the forecast window from 2012 to 2021. This method aims to improve predictive accuracy by incorporating new data into the parameter calibration process, thereby capturing potential non-stationarity in the relationship between the fluxe towards the aquifer and water table elevation. Fig. 7 demonstrates a small improvement in adaptability and temporal accuracy of the forecasts when using the dynamical option. Across different forecast windows and lead times, the model aligns with the observed piezometric elevations, indicating a higher degree of temporal coherence between the recharge signal derived from SEAS5 soil moisture and the groundwater response. Indeed, as confirmed by the performance results in Table 5, although the KGE and the correlation show values similar to those obtained for OPT_1, the RMSE and MAE remain more stable across the various lead times, and their values remain approximately 0.5 m and 0.4, respectively.

The dynamically updated method (OPT_2) produces forecasts that are more tightly clustered together (less uncertain), especially around the middle of the forecast period, lead times 2 to lead time 4 months in Fig. 7b to Fig. 7d. This suggests the model is filtering out random noise and locking onto the real groundwater behavior.

https://doi.org/10.5194/egusphere-2025-3677
Preprint. Discussion started: 6 October 2025

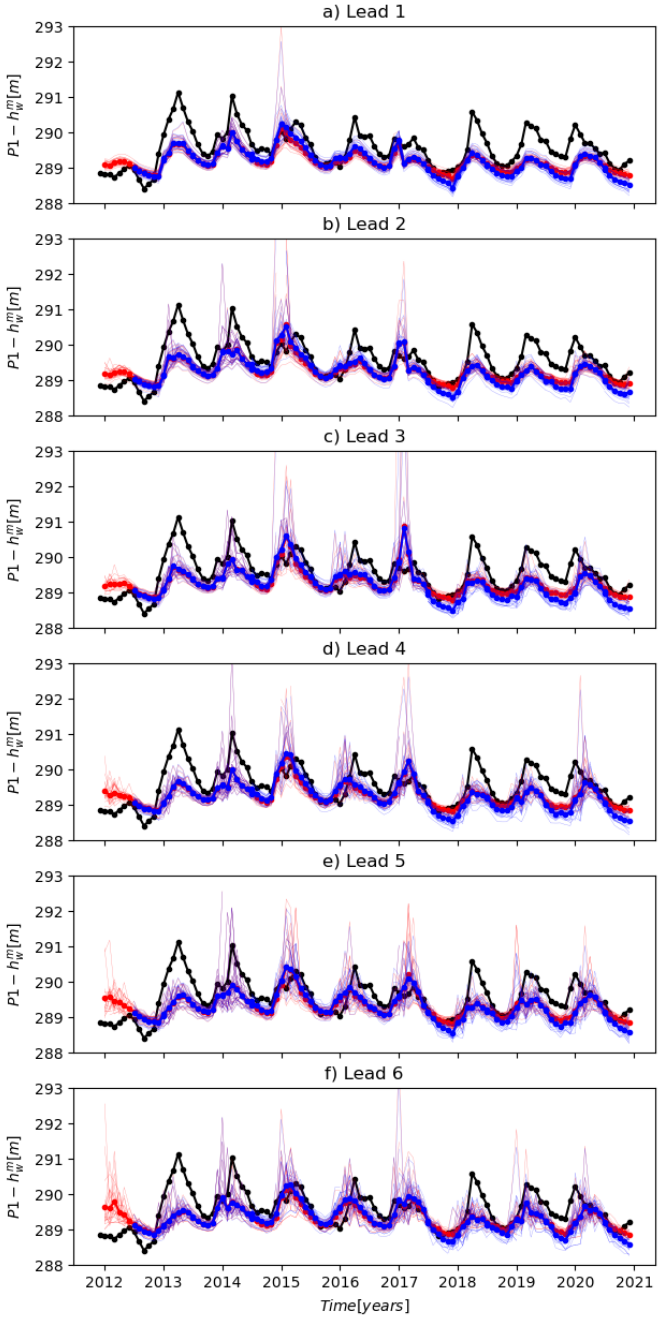

Figure 7. From (a) to (f) the forecast of the monthly water table elevation, h_w^m (in m a.s.l.) of P1-Pistrino piezometer as given by the SEAS5 seasonal forecast (red and black lines indicate the forecasted and measured values, respectively) for each lead time, from 1 month to 6 months. The thick red line is the ensemble average, whereas the thinner ones represent each ensemble member of OPT_1. The thick blue line is the ensemble average, and the thinner ones represent each ensemble member of OPT_2.

https://doi.org/10.5194/egusphere-2025-3677
Preprint. Discussion started: 6 October 2025

In terms of bias and predictive reliability, the dynamic option reduces systematic overestimations or underestimations that were occasionally observed in option #1 (Fig. 4 compared to Fig. 7). This is also confirmed by the results reported in Table 5, with a generally smaller RMSE and MAE values. By frequently updating the calibration parameters, OPT_2 accounts for evolving boundary conditions, such as changes in evapotranspiration efficiency or infiltration dynamics, thereby refining the forecasted response of the aquifer system.

Table 5. Performance parameters of OPT_2.

Piezometer	Lead Time	KGE	RMSE (m)	MAE (m)	R	r^2
P1-Pistrino	Lead 1	0.7	0.5	0.4	0.8	0.7
	Lead 2	0.6	0.5	0.4	0.7	0.7
	Lead 3	0.5	0.5	0.4	0.7	0.6
	Lead 4	0.5	0.5	0.4	0.6	0.6
	Lead 5	0.5	0.5	0.4	0.6	0.6
	Lead 6	0.4	0.5	0.4	0.6	0.5

5 Precipitation influence on seasonal soil moisture

Given the underestimation of the seasonal forecasted water table elevation in certain periods, especially during the winter months, it was decided to verify the precipitation forecast, one of the most significant driving factors influencing seasonal soil moisture anomalies. The monthly cumulative precipitation rate from SEAS5 has been bias-adjusted using ERA5 reanalysis precipitation in the same manner as soil moisture, as explained in the previous sections. A comparison has then been made between the SEAS5 precipitation taken at the point closest to the P1-Pistrino piezometer and that measured at the Pistrino station (weather station, RGU084, in Fig. 2c). At this station, daily precipitation values have been recorded since 1990. The result of the comparison is shown in Fig. 8 and Table 6. Fig. 8 provides a comparative analysis between precipitation anomalies and the observed and forecasted water table elevations as in Fig. 4 for the period 2015 to 2016.

https://doi.org/10.5194/egusphere-2025-3677
Preprint. Discussion started: 6 October 2025

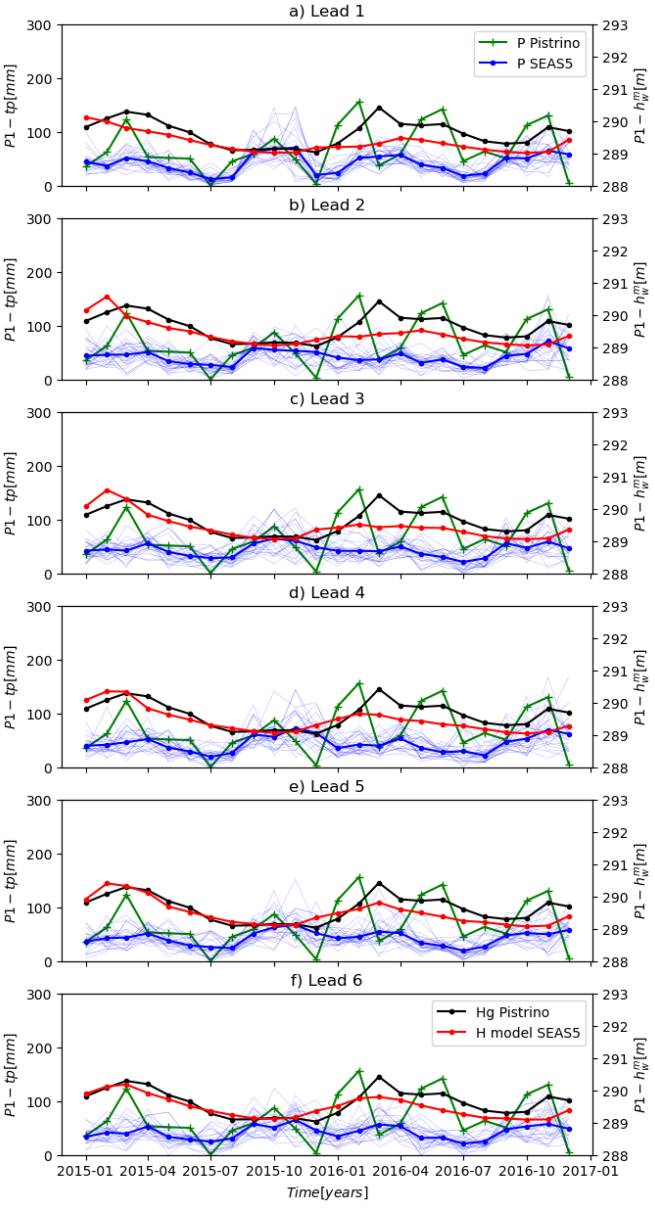

Figure 8. From (a) to (f) the monthly precipitation rate given by SEAS5 compared to the monthly cumulated precipitation of the Pistrino ground-based station (RGU084 in Fig. 2) for each lead time, from 1 to 6 months. A comparison with the monthly water table elevation forecast is offered. The thick blue line is the ensemble average of the precipitation rate, and the others represent each ensemble member, while the green line corresponds to the observed precipitation data. The thick red line is the ensemble average of the predicted water table, the black line is the observed one.

Fig. 8 illustrates seasonal coupling between precipitation patterns and water table elevation. During periods of above-average precipitation, the water table elevation increases; conversely, in drier-than-average periods, water table elevation stationarity

https://doi.org/10.5194/egusphere-2025-3677
Preprint. Discussion started: 6 October 2025

is evident, indicating recharge availability for the aquifer system. Moreover, the soil moisture response to precipitation is not instantaneous but exhibits a lag that increases with soil depth, consistent with the governing principles of vadose zone hydrodynamics. This lag is a key factor in understanding the delayed effect of precipitation on water table elevations, particularly in shallow unconfined aquifers where infiltration is the dominant recharge mechanism.

Table 6. Seasonal forecasts of precipitation performance.

Station	Lead Time	RMSE (m)	MAE (m)	r^2
Pistrino	Lead 1	0.6	0.4	0.3
	Lead 2	0.6	0.4	0.3
	Lead 3	0.6	0.4	0.3
	Lead 4	0.6	0.4	0.3
	Lead 5	0.6	0.4	0.3
	Lead 6	0.6	0.4	0.2

Across all lead times, a general coherence is observed between simulated and observed precipitation, particularly in the seasonal timing of rainfall peaks and dry periods (Figs. 8a to f). This is also shown by the values of the RMSE and MAE reported in Table 6. Both the RMSE and the MAE are stable across all lead times, around 0.6 m and 0.4 m, respectively. These values have been computed considering the forecast period from 2012 to 2020. However, in specific periods, like the one shown in Fig. 8, discrepancies in magnitude and phase become more pronounced as lead time increases. For short lead times (1–2 months, Figs. 8a and b), the SEAS5 system better captures both the intensity and timing of precipitation events, generally resulting in water table elevation forecasts that closely follow the observed piezometric trends. This indicates a strong short-term predictive skill, where accurate rainfall input translates directly into reliable soil moisture dynamics and hence aquifer recharge forecast. The most significant discrepancies between forecasted and observed precipitation are typically found during the autumn and winter months (Fig. 8 for both 2015 and 2016), where the forecasting system often fails to capture high-intensity and short-duration precipitation events. This failure has also been highlighted by previous studies, especially in Mediterranean climates due to limitations in spatial resolution and the representation of convective processes (Seager et al., 2019; Weisheimer et al., 2011). These underestimations or delays in precipitation peaks can lead to under-prediction of recharge, resulting in shallower simulated water table elevations compared to reality. This is particularly noticeable during December 2015, when the seasonal precipitation is not able to forecast the observed trend, resulting in an underestimation of the water table elevation. These extreme events, which are characteristic of the hydrological regime in Mediterranean climates, play a crucial role in groundwater recharge. In summary, Fig. 8 confirms that accurate precipitation forecasts are critical for water table elevation predictability, and that lead-time-dependent uncertainty must be carefully accounted for in operational groundwater forecasting applications. Moreover, this analysis highlights that one of the main limitations of seasonal groundwater forecasting is directly linked to the limited skill in reproducing precipitation, particularly during the autumn and winter months.

https://doi.org/10.5194/egusphere-2025-3677
Preprint. Discussion started: 6 October 2025

6 Discussion and conclusions

This study has demonstrated the feasibility of using bias-adjusted SEAS5 seasonal forecasts in combination with a calibrated nonlinear transfer function to predict water table elevation in shallow unconfined aquifers at seasonal scales. The work stems from the consistent assessment of monthly soil moisture anomalies seasonal forecast skill in the central Mediterranean carried out in Silvestri et al. (2025). Given that a good skill of the soil moisture seasonal forecast was found, they explored the possible application of seasonal forecasts of soil moisture for groundwater management and water table elevation forecast. In their Fig. 14a, the water table elevation observation (expressed as standardized anomalies concerning their mean and standard deviation) in different locations of Italy, including Umbria, were compared with ERA5-LAND reanalysis soil moisture oscillations (Muñoz-Sabater et al., 2021). They showed comparable results between observations and results in terms of soil moisture anomalies. Here we have taken a step toward a direct water table elevation seasonal forecast. More specifically, we have shown the first results of this novel approach for the case study of the P1-Pistrino piezometer in the Umbria region of central Italy.

The results show a good match between forecasted and observed water table elevation, with consistent performance across lead times from 1 to 6 months. The stable values of the statistical indices (RMSE = 0.5 m, MAE = 0.4 m, and KGE >0.4) across options indicate the robustness of the methodology. Notably, the forecasts accurately reproduce seasonal dynamics, particularly during spring and early summer, when recharge processes are primarily governed by soil moisture memory. Furthermore, the narrow ensemble spreads and low forecast biases reported across multiple time windows and initialization months support the feasibility of developing operational groundwater early warning systems based on this methodology (Fig. 5 and Fig. 6).

A key aspect of this study was the comparison between two alternative forecasting options: a static calibration approach (OPT_1), and a dynamically updated method (OPT_2). Both options rely on the same modeling framework, but differ in how frequently the parameters of the groundwater response function are recalibrated. While OPT_1 uses a fixed parameter set derived from a historical reference period (i.e., 2001–2012), OPT_2 introduces time-adaptive recalibration every six months. The results indicate that both methods perform similarly in terms of correlation and overall predictive skill, with OPT_2 showing slightly more stable RMSE and MAE values across different lead times (Table 5). This suggests that the dynamic option can more effectively account for slow, progressive changes in system behavior, such as variations in evapotranspiration, land use, or climate anomalies, without requiring structural changes to the model. Nevertheless, the marginal performance gain observed in the case study implies that the static approach may already be sufficient for relatively stable and homogeneous hydrogeological systems like the Pistrino aquifer. In more complex or heterogeneous settings, however, the adaptive nature of OPT_2 may provide a significant advantage, especially in operational contexts where continuous model updating is feasible. This will be tested in future studies by applying the same option to multiple piezometers in different regions. As mentioned, this second option might be relevant for water resources management. The success of option $\#2$ supports the hypothesis that non-stationarity in the groundwater recharge–response system can be partially mitigated through time-adaptive calibration. The framework presents a promising foundation for operational forecasting systems, especially in regions where external forcings (e.g., land use change, interannual variability in vegetation cover, or climatic anomalies) can alter the groundwater system's memory and response characteristics over time.

https://doi.org/10.5194/egusphere-2025-3677
Preprint. Discussion started: 6 October 2025

However, the analysis also highlights some limitations. First, the skill of water table elevation forecasts is strongly dependent on the quality of precipitation forecasts, as demonstrated by Fig. 8, which shows degradation at longer lead times, especially in autumn and winter. Since the recharge mechanism is strongly driven by precipitation inputs, mediated through soil moisture storage and flux, the degradation in rainfall simulation with lead time directly translates into reduced reliability of the hydrological forecasts. This is a critical issue in Mediterranean regions where groundwater recharge is becoming more dependent on concentrated in short, high-intensity rainfall episodes (Moutahir et al., 2017; Doglioni and Simeone, 2018). As discussed, these events are often underrepresented in SEAS5 due to model limitations in convective parameterization and spatial resolution. Weisheimer and Palmer (2014) and Mastrantonas et al. (2020) noted that ECMWF seasonal forecasts tend to underestimate high-intensity, short-duration events in southern Europe. Lastly, Calì Quaglia et al. (2022) also observed lower forecast skill for precipitation compared to temperature over the Mediterranean basin. Nonetheless, even at longer lead times, the general seasonal trends in the groundwater system are often captured, demonstrating the potential of the approach for anticipatory groundwater management.

It is important to note that one might also consider the possibility of dynamically shifting the calibration period in the proposed option. Instead of simply extending the calibration period by adding the most recent 6 months, one could shift the entire calibration window forward by 6 months, while still maintaining a minimum period of 10 years. This approach may help to better account for the assessed rapid acceleration of climate change (Jenkins et al., 2022). Although in the current case study this does not lead to significantly different results (not shown), we leave this test on a larger set of aquifers with less stable behavior than the one currently analyzed, for future studies.

The novel approach proposed here stands out by directly integrating soil moisture - derived recharge fluxes into a dynamic aquifer response model. Unlike many existing approaches that rely on statistical groundwater forecasting or empirical relationships, this method incorporates physical hydrological processes and operational seasonal forecasts. Especially, the adoption of the dynamic calibration (OPT_2) allows for improved adaptability in non-stationary contexts, making it particularly valuable for water managers operating under evolving environmental and socio-economic conditions. In conclusion, the work presents a promising operational framework for seasonal groundwater forecasting. The coupling of SEAS5 climate forecasts with a calibrated hydrological model offers a reliable tool for anticipatory aquifer management. Future development will not only extend the approach to additional piezometers and aquifer types to assess generalizability, but also will explore the integration of more land surface observations to support forecasting.

Code availability. The Python packages xarray and xskillscore, used extensively in this work, are freely available at https://docs.xarray.dev/en/stable/ and https://xskillscore.readthedocs.io/en/stable/.

https://doi.org/10.5194/egusphere-2025-3677
Preprint. Discussion started: 6 October 2025

Data availability. The ERA5 global reanalysis data and seasonal forecasts can be freely downloaded from the online archive on the Copernicus Climate Data Store system at https://cds.climate.copernicus.eu/datasets. The water table data of Umbria that support the findings of this study are available upon request from https://apps.arpa.umbria.it/acqua/contenuto/Livelli-Di-Falda.

Author contributions. All authors contributed to the conceptualization of the research. G.G. helped with the seasonal forecasting fluxes computation, L.S. carried out the initial model calibration; M.S. carried out the complete seasonal forecasting procedure and the data analysis. All authors contributed to the investigation of the results. M.S. and B.B. wrote the original draft. S.M. and P.B.C. supervised all the research group work. All authors reviewed and edited the manuscript.

Competing interests. no competing interests are present

Acknowledgements. This research has been jointly supported by the University of Perugia *Fondi di ricerca di Ateneo - Edizioni 2021 e 2022*. P.B.C. is financed by the European Union NextGenerationEU under the Italian Ministry of University and Research (MUR) National Innovation Ecosystem grant ECS00000041 - VITALITY (CUP J97G22000170005). M.S. is funded by SSTAM/CIRIAF. L.S. is funded by the Italian Ministry of University and Research (MUR), through the PRIN 2022 PNRR Project P20229KW2R - SEAPLANE - "Simulation and modelling of interface fluxes in wind-wave flows for an improved climate science" (CUP E53D23017010001), within the National Recovery and Resilience Plan (PNRR), Italy, Mission 04 Component 2 Investment 1.1 – NextGenerationEU. Moreover, the Authors would like to thank the project MORE4WATER, which has received funding from MUR (Italy), FCT (Portugal), Fapesc (Brazil), and the European Union's Horizon Europe Programme under the 2022 Joint Transnational Call of the European Partnership Water4All (Grant Agreement n° 101060874).

https://doi.org/10.5194/egusphere-2025-3677
Preprint. Discussion started: 6 October 2025

References

Albergel, C., De Rosnay, P., Balsamo, G., Isaksen, L., and Muñoz-Sabater, J.: Soil moisture analyses at ECMWF. Evaluation using global ground-based in situ observations, Journal of Hydrometeorology, 13, 1442–1460, 2012.

ARPA Umbria: Monitoring of water table elevation in the aquifers of the Umbria Region, Technical report, Agenzia Regionale per la Protezione Ambientale dell'Umbria, Perugia, Italy, http://www.arpa.umbria.it/articoli/il-monitoraggio-continuo-dei-livelli-di-falda-in-u, in Italian, 2008.

Balsamo, G., Beljaars, A., Scipal, K., Viterbo, P., van den Hurk, B., Hirschi, M., and Betts, A. K.: A revised hydrology for the ECMWF model: Verification from field site to terrestrial water storage and impact in the Integrated Forecast System, Journal of Hydrometeorology, 10, 623–643, 2009.

Bongioannini Cerlini, P., Meniconi, S., and Brunone, B.: Groundwater supply and climate change management by means of global atmospheric datasets. Preliminary results, Procedia Engineering, 186, 420–427, 2017.

Bongioannini Cerlini, P., Silvestri, L., Meniconi, S., and Brunone, B.: Simulation of the water table elevation in shallow unconfined aquifers by means of the ERA5 soil moisture dataset. The Umbria region case study, Earth Interactions, 25, 15–32, 2021.

Bongioannini Cerlini, P., Silvestri, L., Meniconi, S., and Brunone, B.: Performance of three reanalyses in simulating the water table elevation in different shallow unconfined aquifers in Central Italy, Meteorological Applications, 30, e2118, 2023.

Brunone, B., Ferrante, M., Romano, N., and Santini, A.: Numerical simulations of one-dimensional infiltration into layered soils with the Richards equation using different estimates of the interlayer conductivity, Vadose Zone Journal, 2, 193–200, 2003.

Brussolo, E., Palazzi, E., von Hardenberg, J., Masetti, G., Vivaldo, G., Previati, M., Canone, D., Gisolo, D., Bevilacqua, I., Provenzale, A., and Ferraris, S.: Aquifer recharge in the Piedmont Alpine zone: historical trends and future scenarios, Hydrology and Earth System Sciences, 26, 407–427, https://doi.org/10.5194/hess-26-407-2022, 2022.

Calì Quaglia, F., Terzago, S., and von Hardenberg, J.: Temperature and precipitation seasonal forecasts over the Mediterranean region: added value compared to simple forecasting methods, Climate Dynamics, 58, 2167–2191, 2022.

De Rosnay, P., Drusch, M., Vasiljevic, D., Balsamo, G., Albergel, C., and Isaksen, L.: A simplified Extended Kalman Filter for the global operational soil moisture analysis at ECMWF, Quarterly Journal of the Royal Meteorological Society, 139, 1199–1213, 2013.

Doglioni, A. and Simeone, V.: Effects of Climatic Changes on Groundwater Availability in a Semi-arid Mediterranean Region, in: IAEG/AEG Annual Meeting Proceedings, San Francisco, California, 2018-Volume 4: Dams, Tunnels, Groundwater Resources, Climate Change, pp. 105–110, Springer, 2018.

Fichefet, T. and Maqueda, M. M.: Sensitivity of a global sea ice model to the treatment of ice thermodynamics and dynamics, Journal of Geophysical Research: Oceans, 102, 12 609–12 646, 1997.

Gupta, H. V., Kling, H., Yilmaz, K. K., and Martinez, G. F.: Decomposition of the mean squared error and NSE performance criteria: Implications for improving hydrological modelling, Journal of Hydrology, 377, 80–91, 2009.

Healy, R. W.: Estimating Groundwater Recharge, Cambridge University Press, 2010.

Hersbach, H., Bell, B., Berrisford, P., Hirahara, S., Horányi, A., Muñoz-Sabater, J., Nicolas, J., Peubey, C., Radu, R., Schepers, D., et al.: The ERA5 global reanalysis, Quarterly Journal of the Royal Meteorological Society, 146, 1999–2049, 2020.

Jenkins, S., Povey, A., Gettelman, A., Grainger, R., Stier, P., and Allen, M.: Is anthropogenic global warming accelerating?, Journal of Climate, 35, 7873–7890, 2022.

https://doi.org/10.5194/egusphere-2025-3677
Preprint. Discussion started: 6 October 2025

Johnson, S. J., Stockdale, T. N., Ferranti, L., Balmaseda, M. A., Molteni, F., Magnusson, L., Tietsche, S., Decremer, D., Weisheimer, A., Balsamo, G., et al.: SEAS5: the new ECMWF seasonal forecast system, Geoscientific Model Development, 12, 1087–1117, 2019.

Kumar, S., Dirmeyer, P. A., and Kinter III, J.: Usefulness of ensemble forecasts from NCEP Climate Forecast System in sub-seasonal to intra-annual forecasting, Geophysical Research Letters, 41, 3586–3593, 2014.

Li, M., Wu, P., and Maand, Z.: A comprehensive evaluation of soil moisture and soil temperature from third-generation atmospheric and land reanalysis data sets, International Journal of Climatology, 40, 5744–5766, 2020.

Lorenz, C. and Kunstmann, H.: The hydrological cycle in three state-of-the-art reanalyses: Intercomparison and performance analysis, Journal of Hydrometereology, 13, 1397–1420, 2012.

Manzanas, R., Gutiérrez, J. M., Bhend, J., Hemri, S., Doblas-Reyes, F. J., Torralba, V., Penabad, E., and Brookshaw, A.: Bias adjustment and ensemble recalibration methods for seasonal forecasting: a comprehensive intercomparison using the C3S dataset, Climate Dynamics, 53, 1287–1305, 2019.

Mastrantonas, N., Magnusson, L., Pappenberger, F., and Matschullat, J.: Extreme precipitation events in the Mediterranean region: Their characteristics and connection to large-scale atmospheric patterns, Tech. rep., Copernicus Meetings, 2020.

Moutahir, H., Bellot, P., Monjo, R., Bellot, J., Garcia, M., and Touhami, I.: Likely effects of climate change on groundwater availability in a Mediterranean region of Southeastern Spain, Hydrological Processes, 31, 161–176, 2017.

Muñoz-Sabater, J., Dutra, E., Agustí-Panareda, A., Albergel, C., Arduini, G., Balsamo, G., Boussetta, S., Choulga, M., Harrigan, S., Hersbach, H., et al.: ERA5-Land: A state-of-the-art global reanalysis dataset for land applications, Earth System Science Data, 13, 4349–4383, 2021.

Seager, R., Osborn, T. J., Kushnir, Y., Simpson, I. R., Nakamura, J., and Liu, H.: Climate variability and change of Mediterranean-type climates, Journal of Climate, 32, 2887–2915, 2019.

Seibert, J., Rodhe, A., and Bishop, K.: Simulating interactions between saturated and unsaturated storage in a conceptual runoff model, Hydrological Processes, 17, 379–390, 2003.

Silvestri, L., Saraceni, M., and Bongioannini Cerlini, P.: Quality management system and design of an integrated mesoscale meteorological network in Central Italy, Metereological Applications, 29, e2060, 2022.

Silvestri, L., Saraceni, M., Brunone, B., Meniconi, S., Passadore, G., and Bongioannini Cerlini, P.: Assessment of seasonal soil moisture forecasts over the Central Mediterranean, Hydrology and Earth System Sciences, 29, 925–946, 2025.

Van Genuchten, M. T.: A closed-form equation for predicting the hydraulic conductivity of unsaturated soils, Soil Science Society of America Journal, 44, 892–898, 1980.

Weisheimer, A. and Palmer, T.: On the reliability of seasonal climate forecasts, Journal of the Royal Society Interface, 11, 20131 162, 2014.

Weisheimer, A., Palmer, T., and Doblas-Reyes, F.: Assessment of representations of model uncertainty in monthly and seasonal forecast ensembles, Geophysical Research Letters, 38, 2011.

WHO: Protecting groundwater for health: Managing the quality of drinking-water sources, IWA Publishing for World Health Organization, 2006.

Zar, J. H.: Spearman rank correlation, Encyclopedia of Biostatistics, 7, 2005.

Zuo, H., Balmaseda, M. A., Tietsche, S., Mogensen, K., and Mayer, M.: The ECMWF operational ensemble reanalysis–analysis system for ocean and sea ice: a description of the system and assessment, Ocean Science, 15, 779–808, 2019.